

Tropical Cyclone Sensitivity to Ocean Coupling

Kristian S. Mogensen, Linus Magnusson
and Jean-Raymond Bidlot

Research and Forecast Department

January 2017

*This paper has not been published and should be regarded as an Internal Report from ECMWF.
Permission to quote from it should be obtained from the ECMWF.*



European Centre for Medium-Range Weather Forecasts
Europäisches Zentrum für mittelfristige Wettervorhersage
Centre européen pour les prévisions météorologiques à moyen terme

Series: ECMWF Technical Memoranda

A full list of ECMWF Publications can be found on our web site under:

<http://www.ecmwf.int/en/research/publications>

Contact: library@ecmwf.int

©Copyright 2017

European Centre for Medium-Range Weather Forecasts
Shinfield Park, Reading, RG2 9AX, England

Literary and scientific copyrights belong to ECMWF and are reserved in all countries. This publication is not to be reprinted or translated in whole or in part without the written permission of the Director-General. Appropriate non-commercial use will normally be granted under the condition that reference is made to ECMWF.

The information within this publication is given in good faith and considered to be true, but ECMWF accepts no liability for error, omission and for loss or damage arising from its use.

Abstract

We present an investigation of the performance of the ECMWF coupled atmosphere-waves-ocean model for different ocean and atmosphere resolutions and coupling strategies on a series of tropical cyclones in the west Pacific with the aim to better understand the coupled feedback mechanisms in these extreme conditions.

For some of the test cases, we only find little impact of coupling the atmosphere to the ocean, while in others, we observe a very large impact. To further understand these differences, we have selected two tropical cyclones as case studies: TC Haiyan (with small impact of coupling) and TC Neoguri (with large impact of coupling). The comparison between these two cases suggests that the upper ocean stratification is the key to determine the strength of the coupled feedback. A strong coupled feedback is found whenever the ocean heat content of the upper layer is low while a very weak coupled feedback is found whenever the ocean has a thick warm mixed layer.

The oceanographic response to tropical cyclones has been compared for the two cases to surface information in the form of sea surface temperature and derived surface currents from drifting buoys and to subsurface observations from Argo and ship launched XBT's. These comparisons show that we are able to realistically reproduce the atmospheric and oceanographic interaction during tropical cyclone conditions which gives us confidence that the coupled modelling system is physically sound.

1 Introduction

Tropical cyclones are one of the deadliest weather phenomena, with TC Haiyan (2013) as a recent reminder leaving more than 6000 people dead. The cyclones give rise to a devastating combination of extreme winds, storm surges, high waves and rainfall. Correctly forecasting severe hurricanes several days in advance make it possible to evacuate the coastlines and prepare the society to the event, as ahead of TC Phalin (2013) when half a million people were evacuated from coastal regions of Odisha and Andhra Pradesh, India. For such actions, the forecast of the cyclone path is essential but also a reliable intensity forecast is needed to give fidelity to the actions.

Historically, the ECMWF forecasts have predicted too weak cyclones and on average this also holds true in recent years ([Haiden et al., 2014](#)). However, in recent years, several cases of too deep cyclones (in terms of central pressure) have occurred in the ECMWF high-resolution (HRES) forecasts. This type of error is now dominating in the north-western corner of the north-western Pacific basin ([Rodwell et al., 2015](#)). The error in this part of the basin is however not unique for ECMWF ([Ito et al., 2015](#)). The issue of too intense cyclones could have many reasons and in this report we will investigate the sensitivity to an interactive ocean model.

The main energy source for tropical cyclones is the heat transport from the ocean. By not coupling the atmosphere and the ocean, the actual feedback from the heat exchange at the surface will be missing and the ocean will act as an infinite source of energy for the atmosphere during the forecast. Using a coupled model introduces a negative feedback between the tropical cyclone and the SST. As strong winds from the cyclone enhance the heat uptake from the ocean, the resulting in a potential cooling of the SST, which in turns reduces the energy available to the cyclone in the next time step. Tropical cyclones interacts with the SST in three ways: the heat transport to the atmosphere (1), vertical mixing (2) and upwelling by Ekman pumping (3). While the first process could be simulated by a slab ocean model, the second requires a mixed-layer model and to simulate all three processes a 3-dimensional model is required, which is important especially for slow moving cyclones ([Yablonsky and Ginis, 2009](#)). The effect of a mixed-layer model in ECMWF low-resolution forecasts (TL159) for tropical cyclones was investigated in [Takaya et al. \(2010\)](#), however the low model resolution led to a negative intensity bias and all cyclones

where relatively weak.

In this report, we will investigate the impact of coupling a relatively high-resolutions (TL1279 (16 km) and TCo1279 (9 km)) atmospheric model to a 3-dimensional ocean model for a selection of tropical cyclone cases in the north-western Pacific. In Section 2 the experiment setup is described together with the verification data. In Section 3 we introduce the selection of tropical cyclones used to investigate the sensitivity and in Section 4 the results from the sensitivity experiments are presented. Finally, in Section 5 the implications of the results are discussed.

2 Model and data

In the present study, we use the operational (in the time of writing) version (CY43R1) of the ECMWF integrated forecasting system (IFS). The IFS contains options to either run with prescribed fields or with an interactive ocean (and sea-ice) model to provide SST and sea ice as input to the atmospheric component. The ocean model used in this setup is based on the NEMO (Madec, 2008) model version 3.4.1 with the LIM2 used as the option for sea-ice with ECMWF modifications to the coupling interface described in Mogensen et al. (2012b).

With an interactive ocean, the model time stepping is such that the atmospheric part of the IFS runs for a number of atmospheric time steps followed by running the oceanographic part of the IFS (NEMO) for a (possibly different) number of oceanographic time steps until the model time is the same for both model systems. This means that the number of time steps of the atmosphere/ocean component multiplied by the atmosphere/ocean time steps needs to be the same and these products represent the coupling frequency of the model. During the atmospheric time steps averaged fluxes, required by the ocean model (*e.g.* heat and momentum), are computed and subsequently passed to the ocean model, which uses them as forcing fields during the ocean time steps. At the end of the ocean time steps, oceanic instantaneous variables (*e.g.* sea surface temperature, surface current and sea ice cover) are passed back to the atmospheric model which concludes a coupling step. For more details on the integrated single executable coupled IFS system see Mogensen et al. (2012b). The single executable system was recently upgraded to also include forcings from the wave model as described in Janssen et al. (2013) and Breivik et al. (2015).

In this study, we have tested a set of configurations of atmospheric resolution, oceanographic resolution and coupling setup. For the atmospheric resolutions, both the current operational resolution (TCo1279, 9 km, described in Wedi et al. (2015)) and the previous operational resolution (TL1279, 16 km) were tested. For the oceanographics resolution, we used both the ORCA1_Z42 configuration (~ 100 km, 10 m top layer) previously used in ensemble prediction system (ENS) in CY41R2 and the new ORCA025_Z75 configuration (~ 25 km, 1 m top layer) implemented with the operational introduction of CY43R1. Since the LIM2 sea-ice model was introduced together with the upgrade of ocean resolution then all runs with ORCA025_Z75 were done with LIM2 switch active to be consistent with this system, but we obviously do not expect this to influence the prediction of the tropical cyclones. The low resolution ocean configuration was only tested with the low resolution atmospheric configuration.

For ocean initial conditions, either the ocean reanalysis system 4 (ORAS4, Mogensen et al. (2012a) and Balmaseda et al. (2013)) for ORCA1_42 or ocean reanalysis system 5 (ORAS5, H. Zuo *et al*, personal communication and Zuo et al. (2015) for an earlier version of ORCA025_Z75 reanalysis) for ORCA025_Z75. For both cases, the reanalysis and not the near-real-time (NRT) ocean initial conditions were used since the NRT stream is not available for ORAS5 for the start dates considered.

The uncoupled simulations were made with persisted anomalies as is currently done in operations for the

high resolution deterministic forecast (HRES). For the TL1279 atmospheric resolution, experiments with OSTIA (Donlon et al., 2012) initial SST (as done for the operational uncoupled forecasts) as well with ORAS4/ORAS5 initial SST were performed in order to have the same initial SST in both coupled and uncoupled mode. For the TCo1279 atmospheric resolution only OSTIA initial SST runs were performed.

The current operational ENS uses a “partial” coupling setup that during the first 4 days of the model integration couples the SST tendencies rather than the actual SST field from the ocean model with a gradual transition to full SST coupling over the next 4 days. This partial coupling is intended to maintain the high spatial variability in the analysed SST in the SST used by the atmosphere in the early part of forecast and to ensure that errors in positions of boundary currents in the ocean analyses do not degrade the atmospheric forecast. In the present study, we have tested the effect of using this scheme as well as doing the full coupling of the SST predicted by the ocean. For more details on the partial coupling please see Janssen et al. (2013).

A summary of the experiments performed can be found in table 1.

Experiment	Atmosphere	Coupling	Ocean	Oce. Init.	LIM2 active	SST source
gji8	TL1279	Full	ORCA025	ORAS5	Yes	
gji9	TL1279	Full	ORCA1	ORAS4	No	
gjia	TL1279	Partial	ORCA025	ORAS5	Yes	
gjib	TL1279	Partial	ORCA1	ORAS4	No	
gjid	TL1279	None				ORAS5
gjic	TL1279	None				ORAS4
gjie	TL1279	None				OSTIA
gjix	TCo1279	Full	ORCA025	ORAS5	Yes	
gjyy	TCo1279	Partial	ORCA025	ORAS5	Yes	
gjiz	TCo1279	None				OSTIA

Table 1: Settings for the different experiments.

The position and intensity of tropical cyclones are subjectively assessed by meteorologists at tropical cyclone warning centres using all available observations, and the estimate is put into the “Best Track” database (Knapp et al., 2010; Levinson et al., 2010). A main source of information here are visible and infrared satellite imagery that are used to estimate the intensity of cyclones by the Dvorak technique (Dvorak, 1975; Velden et al., 2006). The errors in the intensity estimation using the Dvorak technique in comparison to aircraft measurements was investigated in Martin and Grey (1993) and more recently the uncertainty in the Best Track database was investigated by Landsea and Franklin (2013).

3 Test cases

In recent years (2013 and 2014), the monitoring of tropical cyclones has highlighted a difference in the intensity errors between the northern and southern part of the north-western Pacific basin (see Rodwell et al. (2015)). While the southern part is clearly dominated by negative intensity error (too weak cyclones), positive intensity error (too strong cyclones) dominates the northern part of the basin. However, the sample in the northern part of the basin is dominated by more mature cyclones that are typically larger in size. Another difference between the northern and southern part is the ocean heat content and depth of the very warm layer (colder and shallower in the north). Therefore, it is not straight forward to isolate one key reason for the over-deepening of the cyclones by stratifying the results.

In order to run sensitivity experiments for tropical cyclones, we have selected 8 cases in the north-western Pacific from the seasons 2013 and 2014 (Table 2). The selection is not aimed to cover all types of cyclones but to investigate the contrast in error between the southern and northern part of the basin. All cases chosen had a low track error to let us to focus on modelling of intensity.

The three panels in Figure 1 show maps of the central pressure for all forecast steps during the first 5 days (left for TL1279 uncoupled runs, middle for the TCo1279 uncoupled runs) and the corresponding BestTrack central pressures (right). In this selection of cases, the forecasts have the cyclones with the lowest central pressure in the north-western part of the basin and the cyclones in the southern part are the weakest. For the Best Track estimates it is the opposite: the cases in the south are the strongest (dominated by Haiyan), while the cases in the north-western part are relatively weak.

For all cases, 3 initial dates were selected for the forecasts. The dates are chosen to be during the first days of the cyclone to let the model spin-up the cyclones. In total this makes 24 forecasts cases.

Name	Start	End	Lowest pressure	Landfall
SOULIK (2013)	2013-07-08 00 UTC	2013-07-14 00 UTC	925 hPa	Taiwan
USAGI (2013)	2013-09-16 18 UTC	2013-09-23 06 UTC	910 hPa	S. China
FRANCISCO (2013)	2013-10-16 06 UTC	2013-10-26 06 UTC	920 hPa	-
HAIYAN (2013)	2013-11-04 00 UTC	2013-11-11 06 UTC	895 hPa	Philippines
NEOGURI (2014)	2014-07-03 18 UTC	2014-07-11 00 UTC	930 hPa	Japan
HALONG (2014)	2014-07-29 00 UTC	2014-08-11 00 UTC	920 hPa	Japan
VONGFONG (2014)	2014-10-03 12 UTC	2014-10-14 00 UTC	900 hPa	Japan
HAGUPIT(2014)	2014-12-01 00 UTC	2014-12-11 06 UTC	905 hPa	Philippines

Table 2: Test cases for tropical cyclones.

4 Results

4.1 All cases

Figure 2 (top panels for TL1279, middle panels for TCo1279) shows the maps of intensity error for all cases (in total 24 forecasts) and forecast steps 24 to 120 hours with 6 hours increments. For the uncoupled experiment (Figures 2(a) and 2(b)) we find too weak cyclones in the southern part of the basin (positive pressure error) and too intense cyclones in the north-west (negative pressure error). Figures 2(c) and 2(d) shows the same but for the fully coupled experiments (the differences between the coupled/uncoupled experiments are plotted in Figures 2(e) and 2(f)). For the coupled experiment the central pressure is increased for most of the cases in north-western part of the basin resulting in reduced errors, while the effect of the coupling is small in the southern part of the basin. This is desirable as the cyclones are already too weak in this part and a further weakening would increase the error.

Figure 3 shows a scatter plot of forecast central pressure vs. Best Track central pressure for the same set of data as in Figure 2. In the figure the uncoupled runs starting from OSTIA are shown. Compared to the uncoupled (left), the fully coupled (middle) and partially coupled (right) forecasts have much fewer cases with large negative pressure errors, as expected from the maps above.

For cases of very deep observed center pressures, there is an obvious improvement with increased atmospheric resolution even though the model is still not able to properly predict very deep intense tropical cyclones. However with the increased atmospheric resolution the over prediction of the uncoupled model

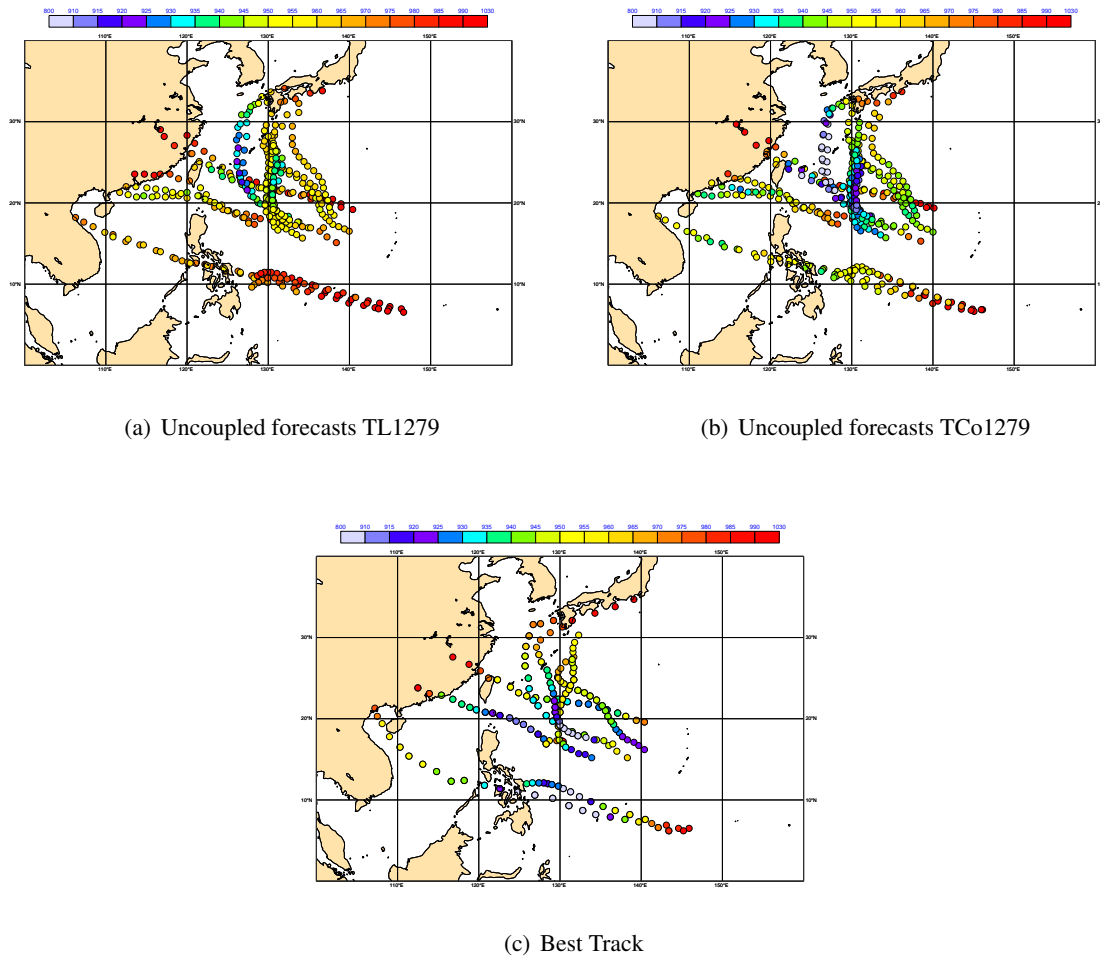


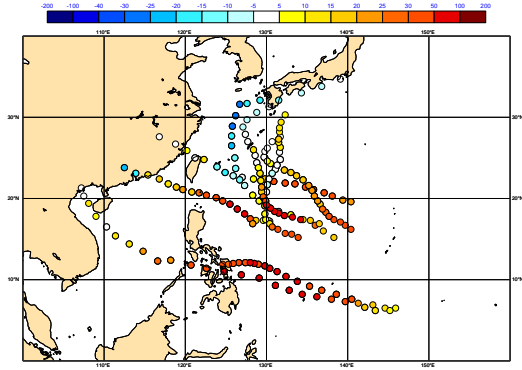
Figure 1: Minimum pressure (hPa) for all cases and all forecast steps between 24 and 120 hours for the uncoupled experiments with OSTIA SST (as in operations).

runs for some cases gets larger and the effect of coupling to reduce these over predictions becomes even larger. It is encouraging to observe that the coupling does not seem to cause an increase in cases where the model under predict the strength of the tropical cyclones.

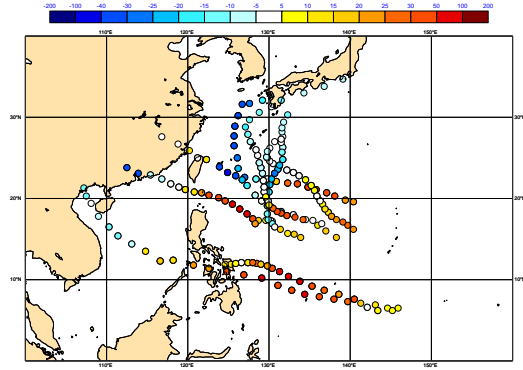
We also notice that two cases stand out from the others: Haiyan is severely underpredicted (≈ 60 to 80 hPa) for all experiments and Neoguri is overpredicted for the uncoupled experiments with an overprediction (≈ 50 hPa) for the TCo1279 atmospheric resolution. We will discuss those two cases in more details in section 4.3.

4.2 Effect of initial SST on uncoupled forecasts

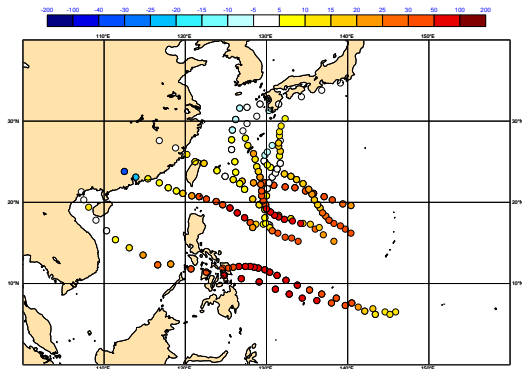
Since the coupled model runs use the initial SST from a 3D ocean analysis state and the uncoupled model runs use a prescribed SST from a 2D analysis from OSTIA the difference in coupled versus uncoupled model performance could partly originate from differences in initial SST. On Figure 4 similar plots to Figure 3 are shown for different uncoupled runs with different initial SST and with the same persisted anomaly scheme. The fact that the runs with SST from ORAS4 have less over prediction in the northern



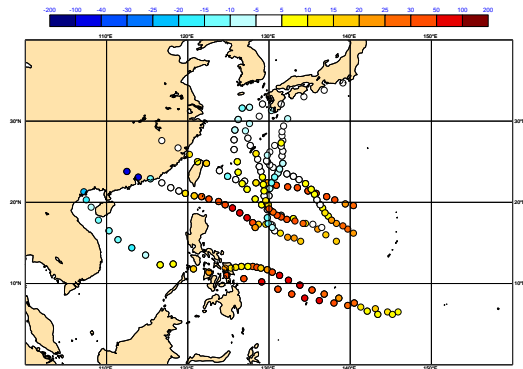
(a) Uncoupled-Best Track TL1279



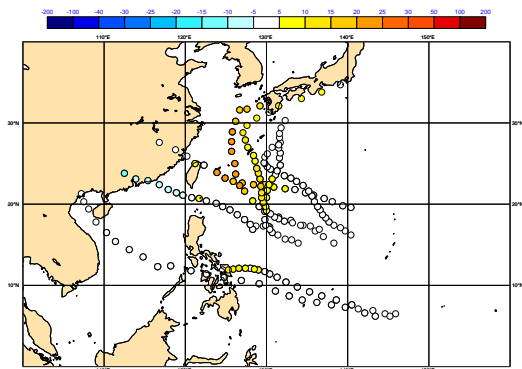
(b) Uncoupled-Best Track TCo1279



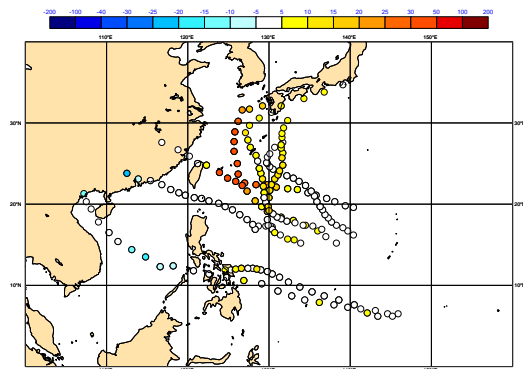
(c) Fully coupled-Best Track TL1279



(d) Fully coupled-Best Track TCo1279

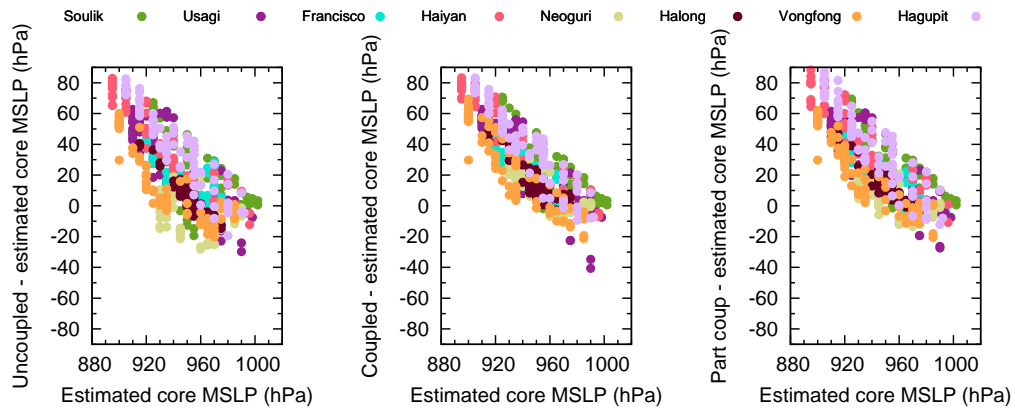


(e) Fully coupled-Uncoupled TL1279

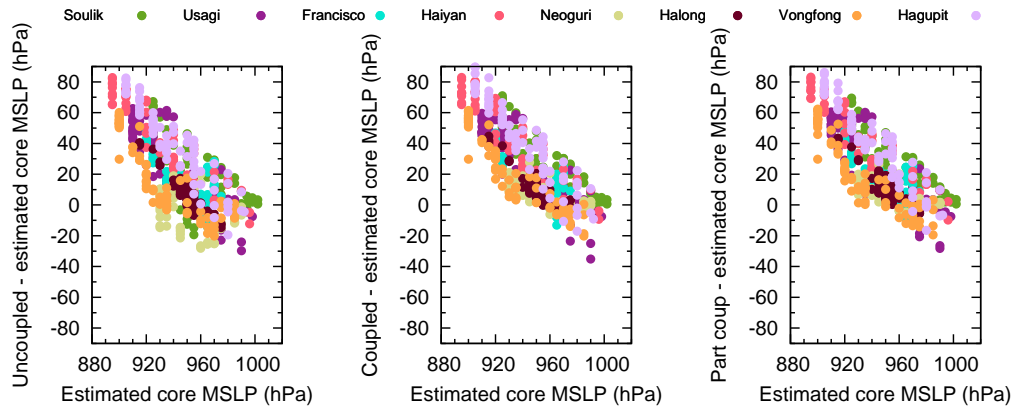


(f) Fully coupled-Uncoupled TCo1279

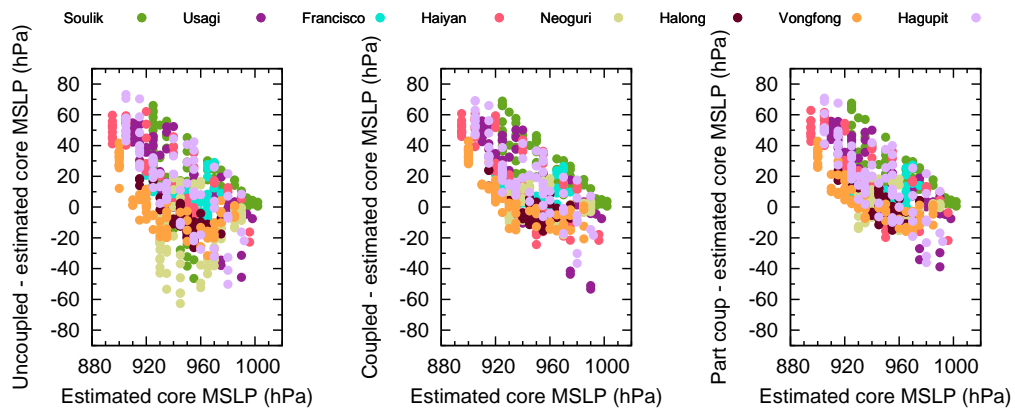
Figure 2: Minimum pressure errors (hPa) for all cases and all forecast steps between 24 and 120 hours.



(a) TL1279 ORCA1



(b) TL1279 ORCA025



(c) TCo1279 ORCA025

Figure 3: Minimum pressure errors for the uncoupled (left) and coupled (middle) and partially coupled (right) forecasts for all cases and all forecast steps between 24 and 120 hours for different atmospheric and oceanographic resolutions. Each individual storm is shown with a different colour.

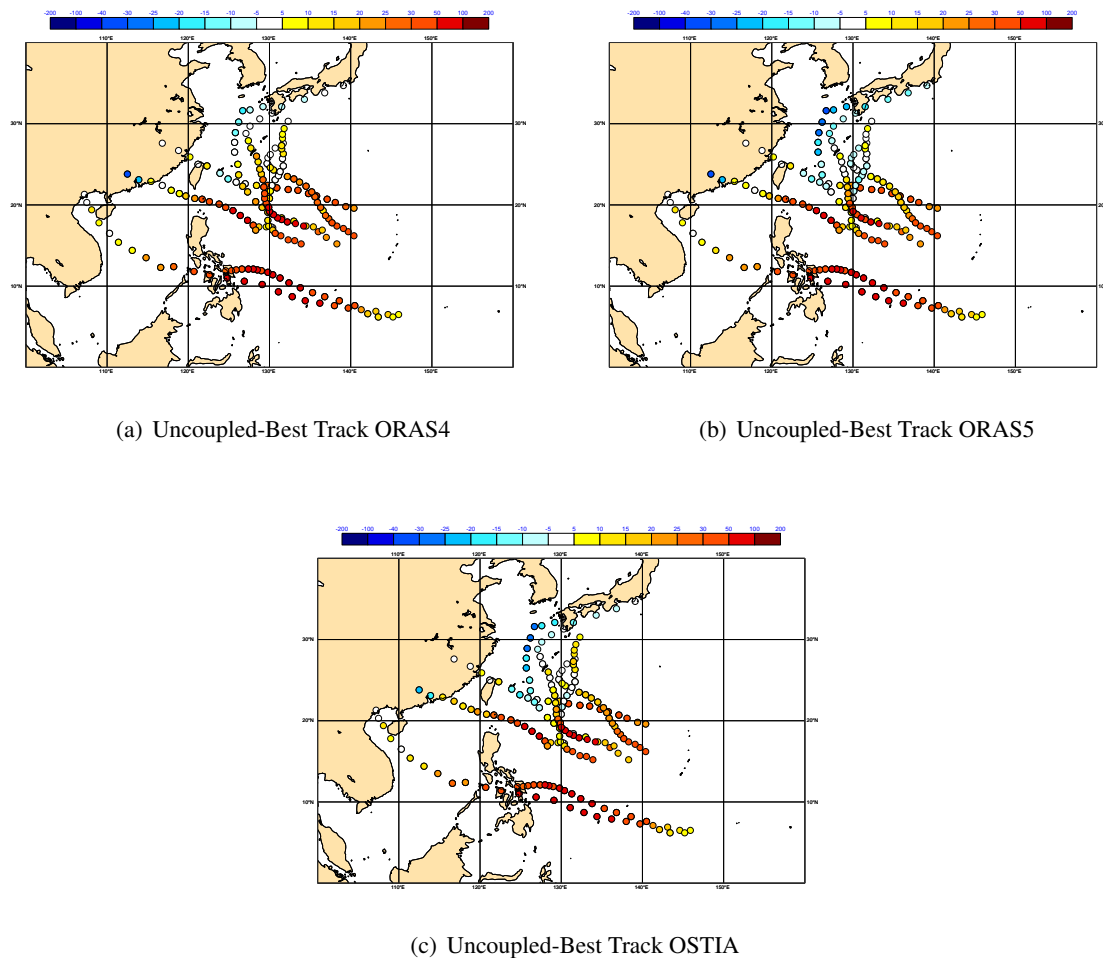


Figure 4: Minimum pressure errors (hPa) for all cases and all forecast steps between 24 and 120 hours for the uncoupled TL1279 experiments for the initial SST from ORAS4 (left), ORAS5 (middle) and OSTIA (right).

part of the basin is due to the fact that the ORAS4 has a thicker top layer than ORAS5 and is therefore expected to be colder in areas with a steep thermocline. The runs based on ORAS5 and OSTIA SST's (middle and right on the figure) are very similar, so the main difference seen in the northern part of the basin in Figure 3 can be accredited to the coupling and not to differences in initial SST.

4.3 TC Haiyan (2013) and TC Neoguri (2014)

To further understand the results from the previous section, we will in this section focus on the two most extreme cases in terms of ocean coupling impact: Haiyan in the southern part of the basin with only a small impact from the coupling and Neoguri with the strongest impact among all the cases. Figures 5 and 6 show the position and central pressure for the forecast (square) and Best Track (triangles) for the first 5 days of one of the forecasts for each case. For both cases, the predicted tracks agree well with the observed ones for all combinations of atmospheric resolutions and coupled/uncoupled setups. Regarding the intensity, both uncoupled/coupled experiments for Haiyan predict a too weak cyclone but with only a small difference in-between them. For Neoguri, the uncoupled forecasts have a too intense cyclone

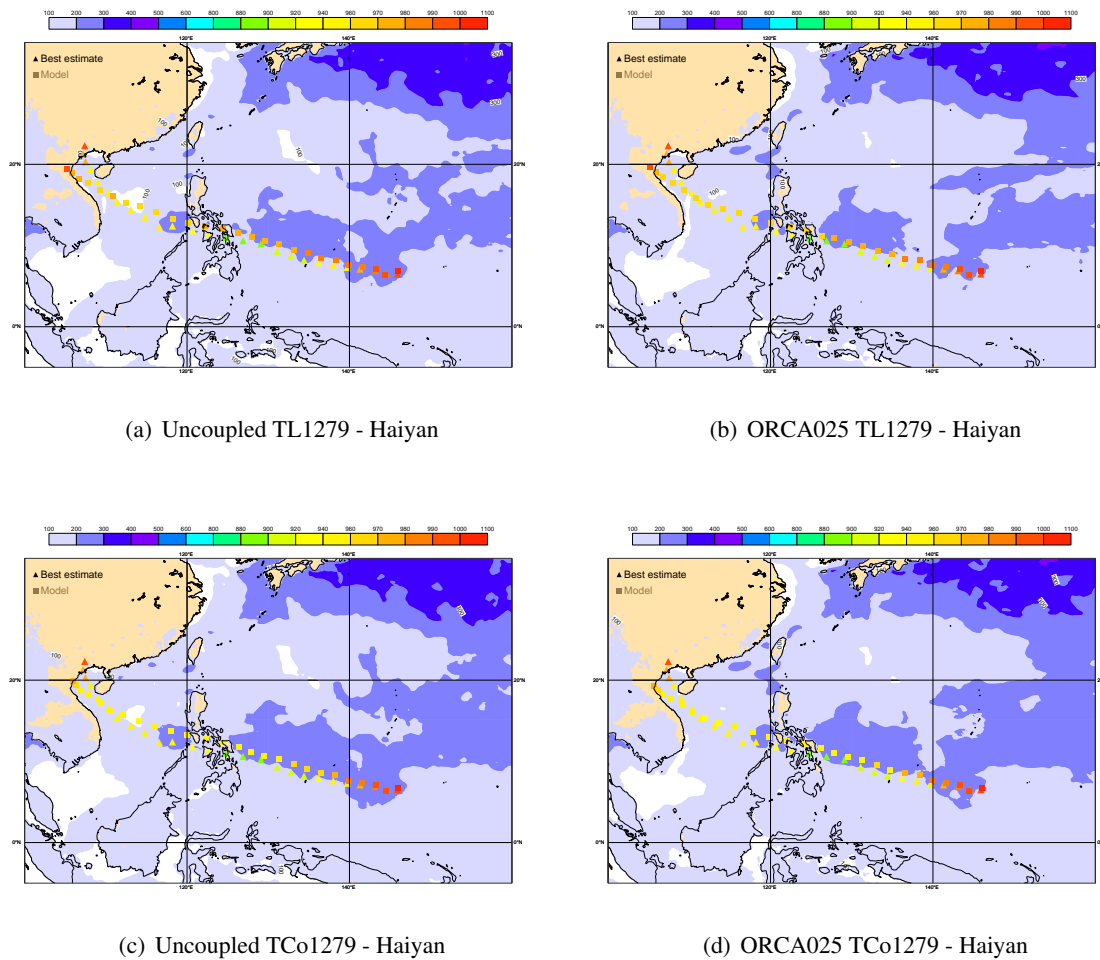


Figure 5: 5-day accumulated net surface heat-flux (sensible + latent) in W/m^2 (shades) from 2013-11-05 (Haiyan). Minimum pressure (in hPa) in the forecast (squares) and Best Track (triangles).

for forecast day 3-5, while the coupled forecasts is better at this range. The panels also include the net surface heat-flux (sensible + latent) to the atmosphere averaged over 5 days. For Haiyan there is little trace in the heat-flux in the wake of the cyclone while for Neoguri we find increased heat-flux from the ocean in the uncoupled forecasts especially for the TCo1279 atmospheric resolution.

Figure 7 shows comparison between uncoupled (cyan for TL1279, yellow for TCo1279,) and coupled (red for TL1279+ORCA025, green for TL1279+ORCA1, blue for TCo1279+ORCA025) forecasts of the evolution of the net (sensible+latent) heat flux averaged over 6 hours in a radius of 150km around the centre of the cyclone (top) and the central pressure (bottom) for Haiyan (left) and Neoguri (right). The plots include all 3 initial dates for each case. All experiments produce similar heat-fluxes for Haiyan, while for Neoguri the heat-flux for the uncoupled forecast is almost twice compared to the coupled forecast during the most intense stage of the cyclone.

For the central pressure, Haiyan represents a cyclone where the intensity was underestimated and Neoguri represents a case where the intensity was overestimated in its latter stage for the uncoupled forecasts (similar to operations) as was also shown on Figure 5 for the 2013-11-05 start date and Figure 6 for the 2014-07-05 start date. While the effect of the coupling is small for Haiyan, the intensity is much

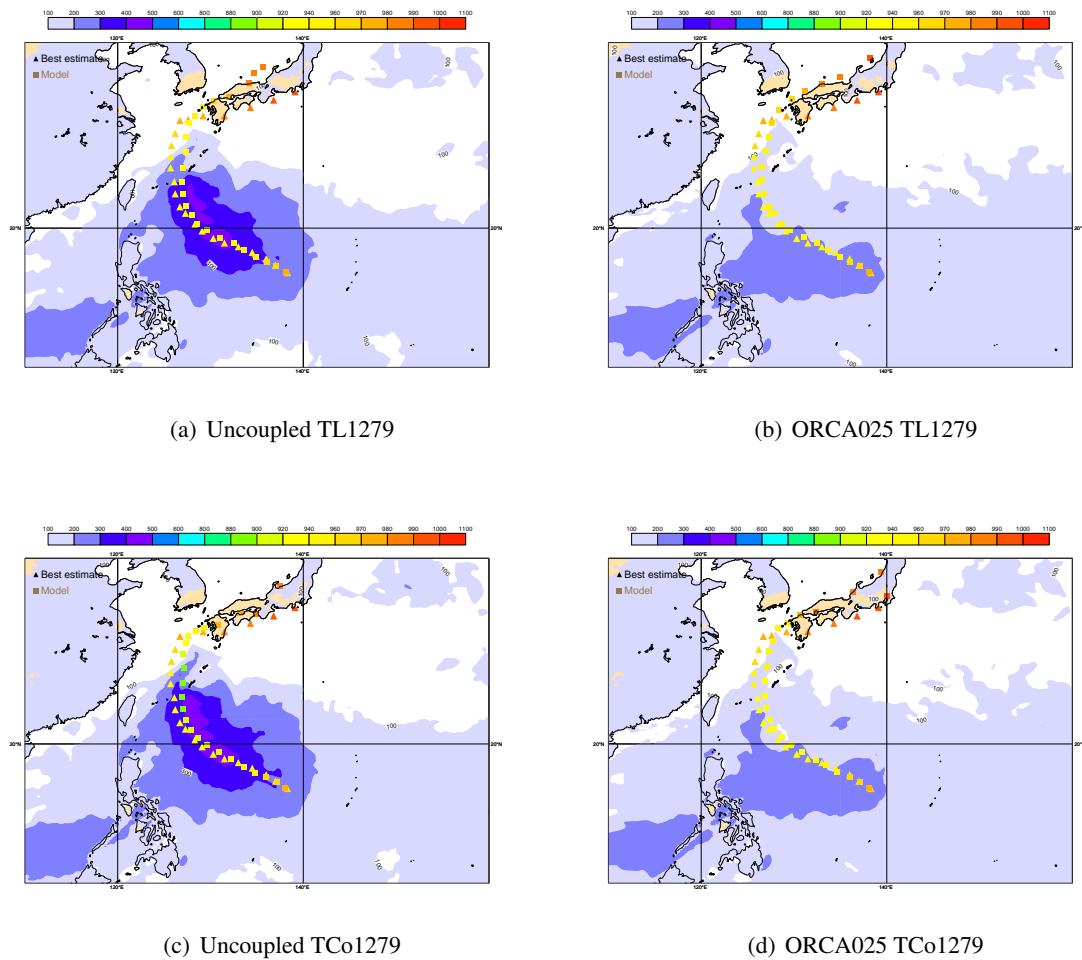


Figure 6: 5-day accumulated surface heat-flux (sensible + latent) in W/m^2 (shades) from 2014-07-05 (Neoguri). Minimum pressure (in hPa) in the forecast (squares) and Best Track (triangles).

reduced in the Neoguri case. The increase in atmospheric resolution for TL1279 to TCo1279 increases the intensity in the forecasts of Haiyan slightly, but the forecasts are still too weak. For Neoguri the increase in atmospheric resolution leads to an even stronger overestimate of the intensity in the uncoupled runs, but with coupling active the differences between the atmospheric resolution becomes much smaller but with a clear improvement in the intensity with the higher atmospheric resolution.

4.3.1 Comparison with observations of SST from drifting buoys

Figures 8 (Haiyan) and 9 (Neoguri) show the SST in 5-day forecasts in uncoupled (top left) and coupled (3 other panels) model and observations of SST at the verification date. By construction, we do not find a cold wake in the uncoupled experiment as it uses SST anomalies from the analysis time.

There is no clear trace of a cold wake after Haiyan, neither in the coupled forecast nor in the (few) observations available. The opposite holds true for Neoguri where we find a strong cold wake in the coupled forecasts. The effect of the coupling reaches 5K in the wake of the cyclone, which is in line with

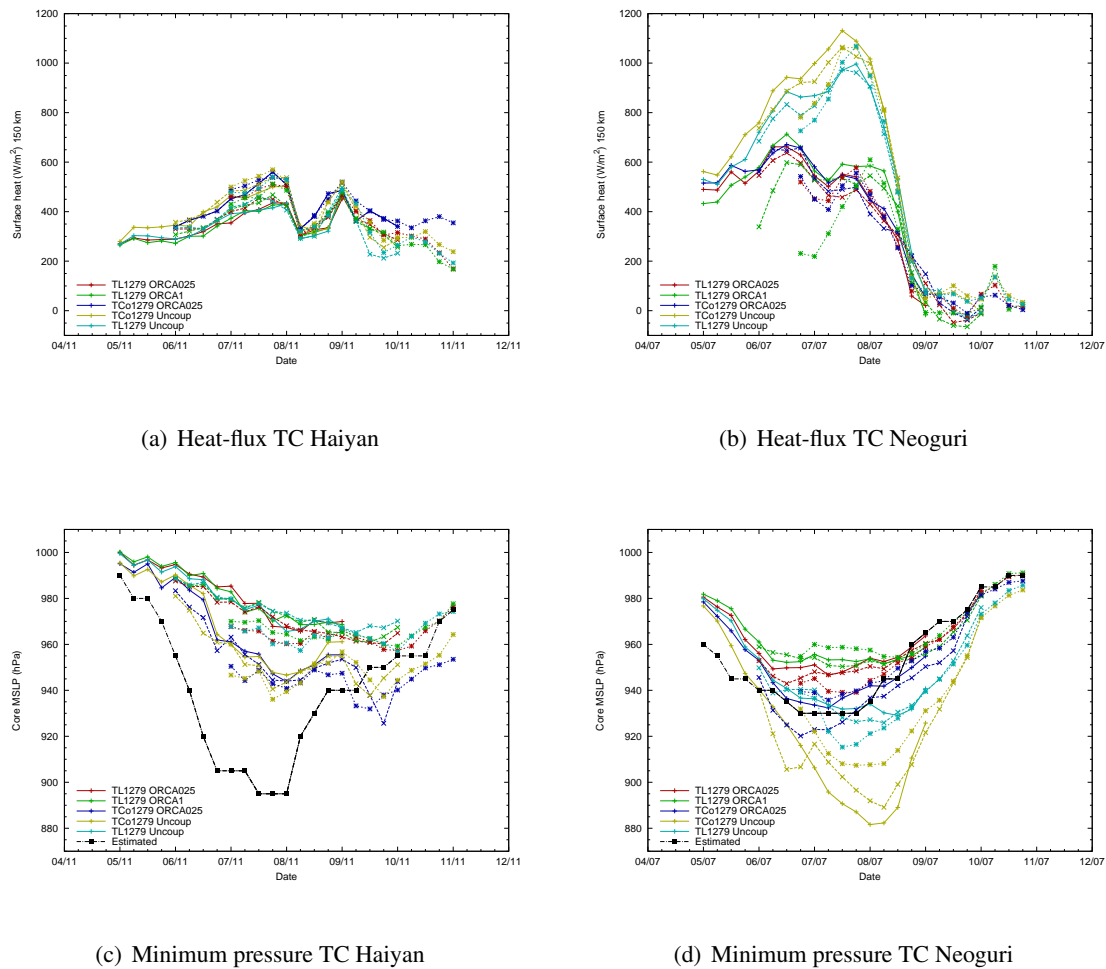


Figure 7: Surface net (sensible+latent) heat flux (top) and central pressure (bottom) for TC Haiyan and TC Neoguri. Best Track (black), uncoupled model (blue) and coupled model (red). Different initial dates are plotted with different line styles.

studies for other cyclones in the literature (Sakaida et al., 1998; Wada et al., 2014; Halliwell et al., 2015; Heo et al., 2017). The SST in the coupled forecasts is in good agreement with the two observations inside the wake of the cyclone. To further quantify this agreement Figure 10 shows the time series of 4 drifting buoys (DRIBU) in the vicinity of the path of Neoguri. For the DRIBU (52514) with the strongest effect, the evolution of the SST in the coupled forecast agrees well with the observation, which also shows a cooling of 5 K over 24 hours. For this particular observation, the TCo1279 coupled model seems to perform slightly better, which is consistent with the improvement in the intensity forecasts mentioned earlier (see Figure 7(d)). For the buoys (52820 and 52596) reached by the typhoon close to the initial time of the forecasts, the results are more mixed. For 52820, the response is not strong enough which is consistent with the model not deepening the cyclone fast enough in the early part of the forecast. However for 52596, the model overpredict the cooling with the high resolution ocean, but the magnitude of the cooling is smaller for this buoy. For 21973 on the right hand side of the cyclone, the model seem to also overpredict the cooling, but for this observation close to the fringe of the cooling the exact path of the predicted tropical cyclone becomes an issue and we do see a slight track error with the predicted track being too close to the position of 21973 (see Figure 6(d)). Overall the conclusion is that the cold

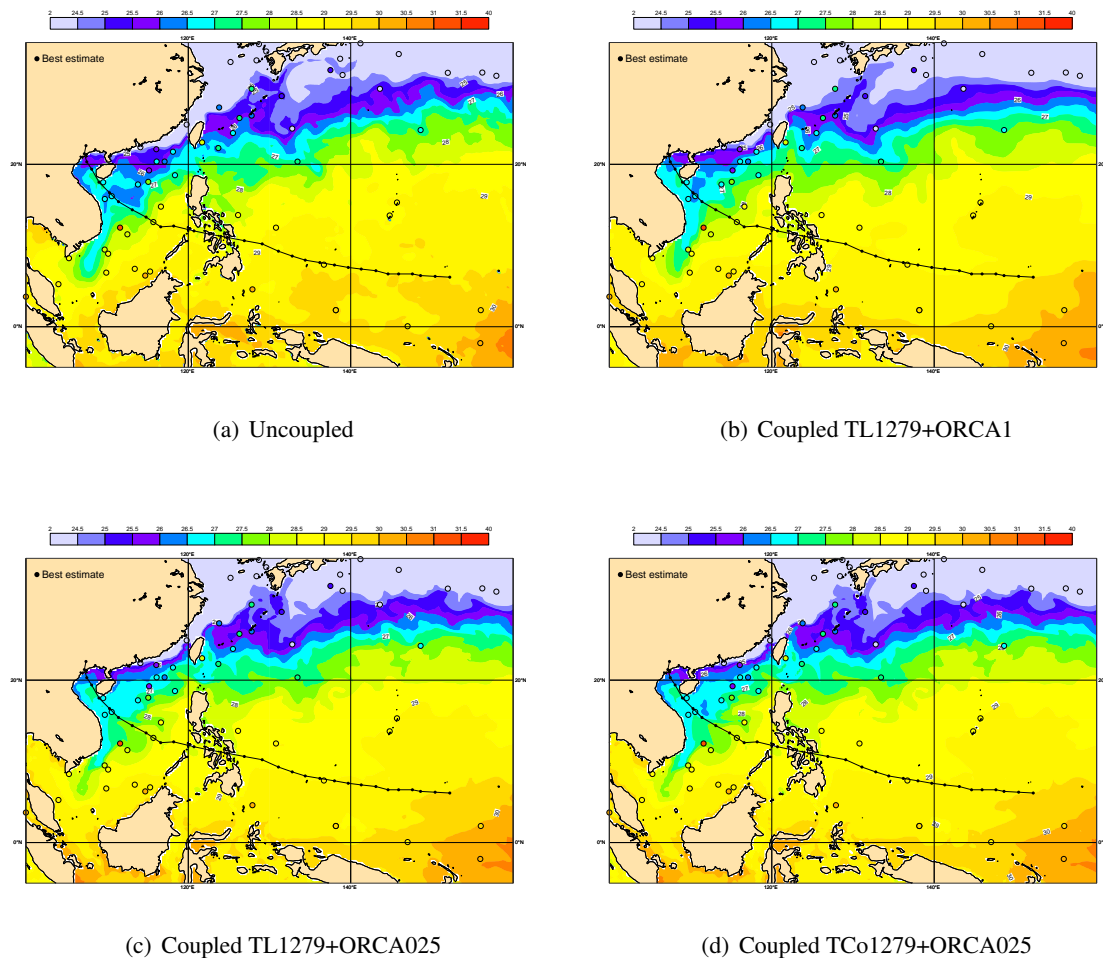


Figure 8: 5-day SST forecast (shades) from 2013-11-05 and SST observations 2013-11-09 00 UTC (symbols)

wake predicted by the coupled IFS model is in reasonable agreement with observations. It is also worth noting that the coupled model develops a diurnal cycle in the SST after the clouds have cleared which by construction is not present in the uncoupled model.

4.3.2 Sub-surface oceanic response and comparison with observations

The small effect of the coupling for Haiyan could be connected to the deep and well developed ocean mixed-layer for this case (Lin et al., 2014), but it could also be due to the fact that the weak cyclone in the forecast is not able to increase the heat-flux. In order to investigate this further together with the strong effect of the coupling for Neoguri, we will now look at the sub-surface response in the ocean in the two cases. Figure 11 shows times series for temperatures and 3D currents for the point on the model track closest to the estimated Haiyan Best Track position the 7th of November 2013 at 00 UTC. A similar plot for Neoguri for the 7th of July 2014 at 18 UTC is shown on Figure 12. The points were chosen to reflect the response in the open ocean. Other nearby points (and the different start dates) for the two cases shows very similar behaviour.

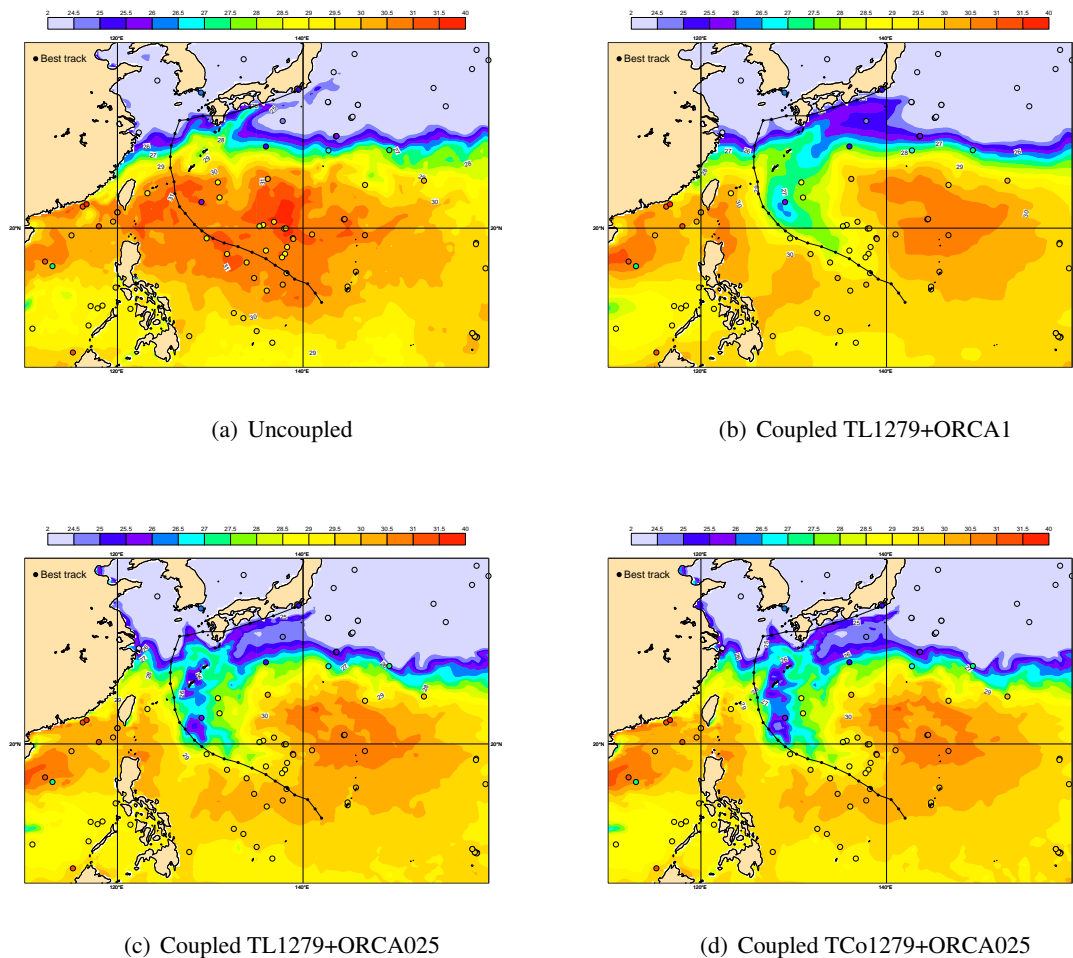
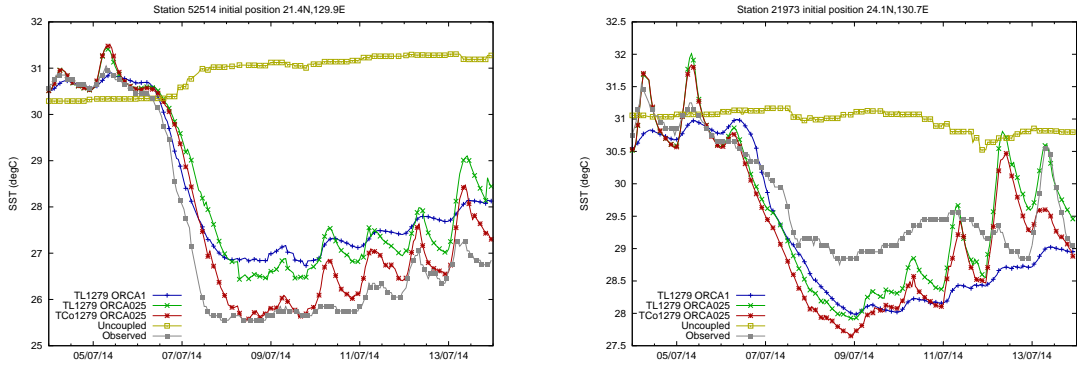


Figure 9: 5-day SST forecast (shades) from 2014-07-05 and SST observations 2014-07-09 00 UTC (symbols)

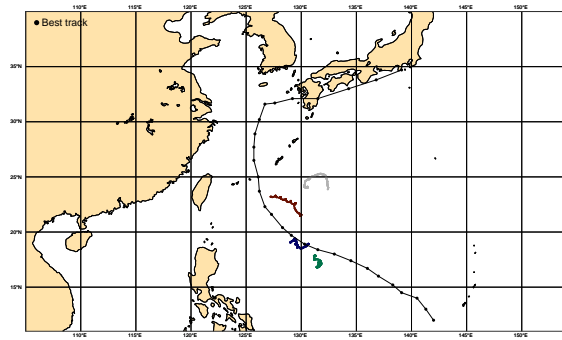
Looking at the temperature at initial time for the Haiyan case (Figure 11 top), it is clear that the ocean has a deep (≈ 80 m) layer of warm water whereas for the Neoguri case the thermocline is steeper, so even though the temperature at the surface is higher, the heat content in the surface region is lower for the Neoguri case. When the tropical cyclone reaches the point (after 3 days for Haiyan and 3.75 days for Neoguri) the response is quite different. For Haiyan there is a small cooling (not really visible on the plot) of the whole of the thick warm layer whereas for Neoguri the shallow warm layer is depleted of heat causing the large cooling of ocean temperature in the upper ocean. These results are in qualitative agreement with observational investigations by [Lin et al. \(2008\)](#); [Lin and Pun \(2009\)](#) and supports the conclusion that the ocean stratification is the main driver for the magnitude of the coupled feedback. The temperature response for Neoguri is stronger with increasing atmospheric and oceanographic resolution, but the basic signature of cooling for the first 20 meters are present even for the TL1279/ORCA1 combination.

For Haiyan, we can compare the evolution of the sub-surface temperature at the point used in Figure 11 to observations from Argo floats since several observations are available near this point during the period of the typhoon. Such a comparison is shown in Figure 13 which shows the observations closest (and not more than 250 km away) to the position 8.7N,132.8E and model output interpolated to the observation

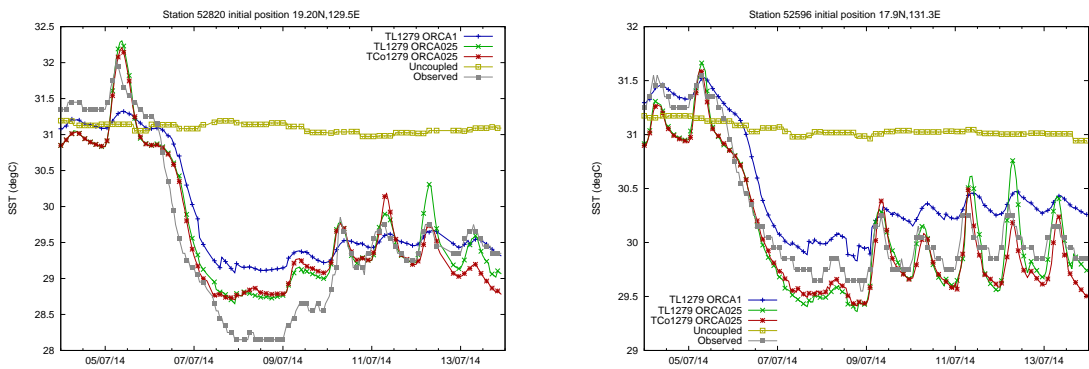


(a) DRIBU 52514 (brown on map)

(b) DRIBU 21973 (grey on map)



(c) Positions



(d) DRIBU 52820 (blue on map)

(e) DRIBU 52596 (green on map)

Figure 10: SST forecasts and observations from 4 DRIBU for the Neoguri case for the different atmospheric and oceanographic resolutions.

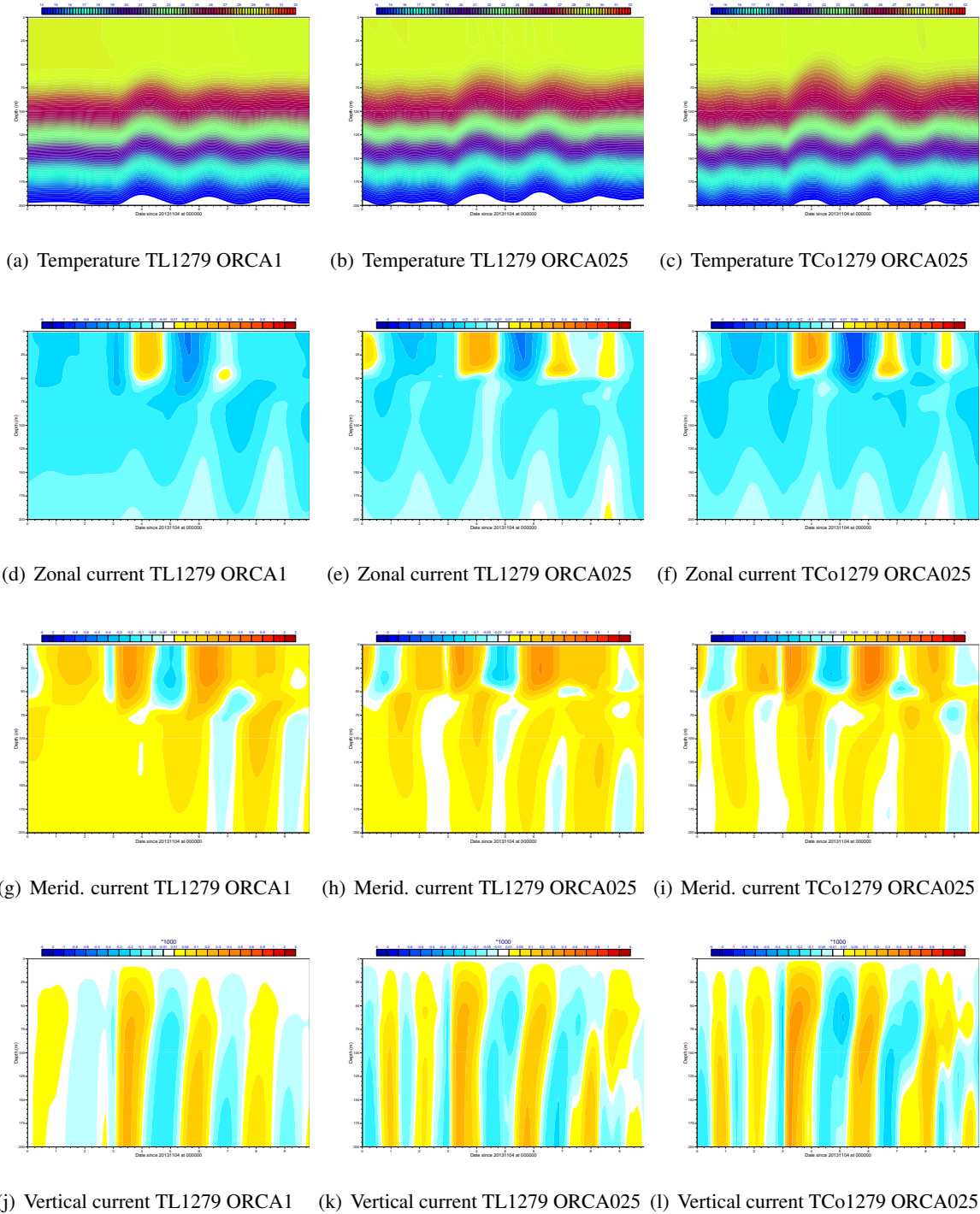


Figure 11: Vertical time series for Haiyan coupled simulations for temperature, zonal current, meridional current and vertical current for the model cyclone position nearest to the estimated 8.7N,132.8E position at 2013-11-07 00 UTC valid time for different atmosphere/ocean resolutions pairs (columns).

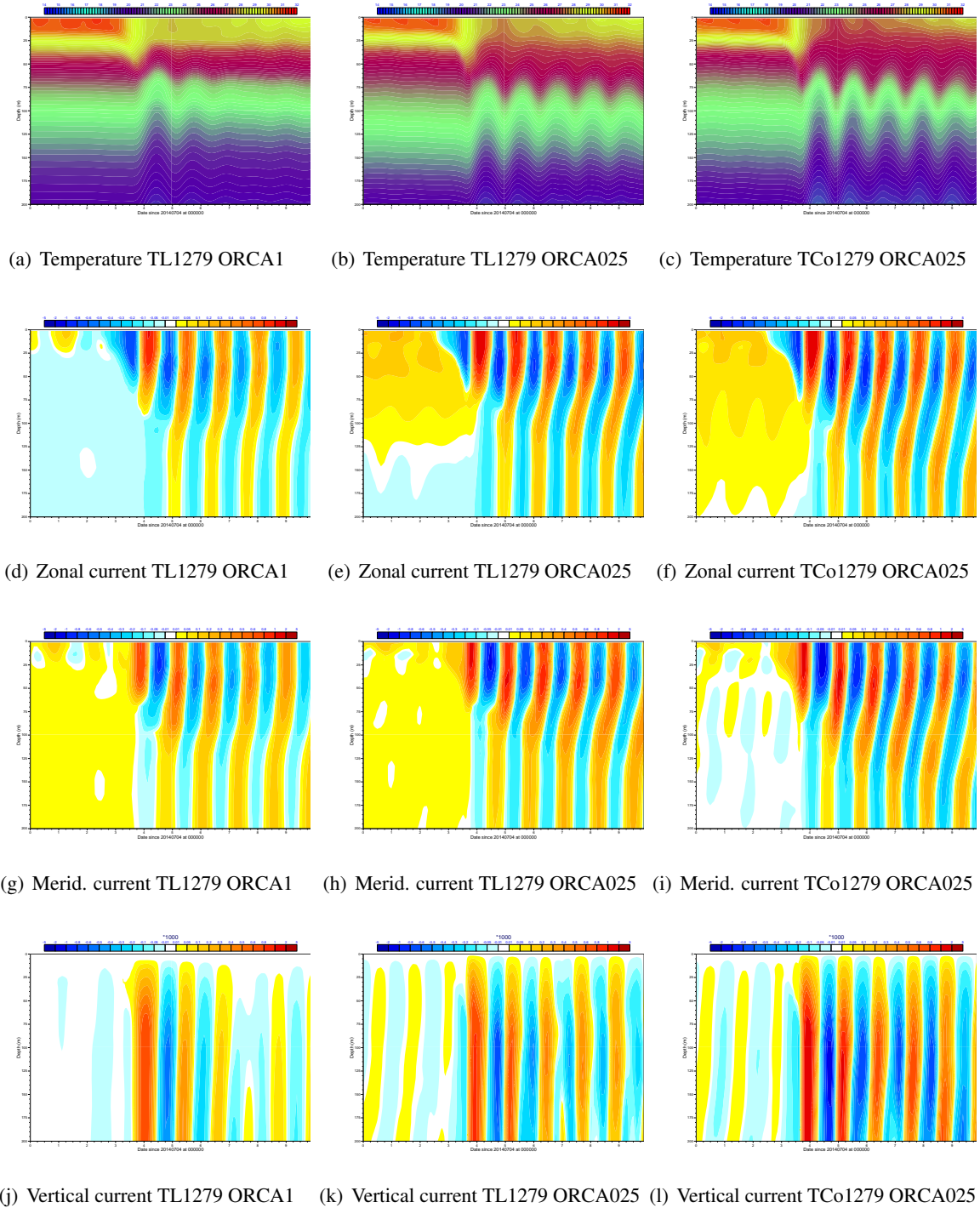


Figure 12: Vertical time series for Neoguri coupled simulations for temperature, zonal current, meridional current and vertical current for the model cyclone position nearest to the estimated 23.7,126.2E position at 2014-07-07 18 UTC valid time for different atmosphere/ocean resolutions pairs (columns).

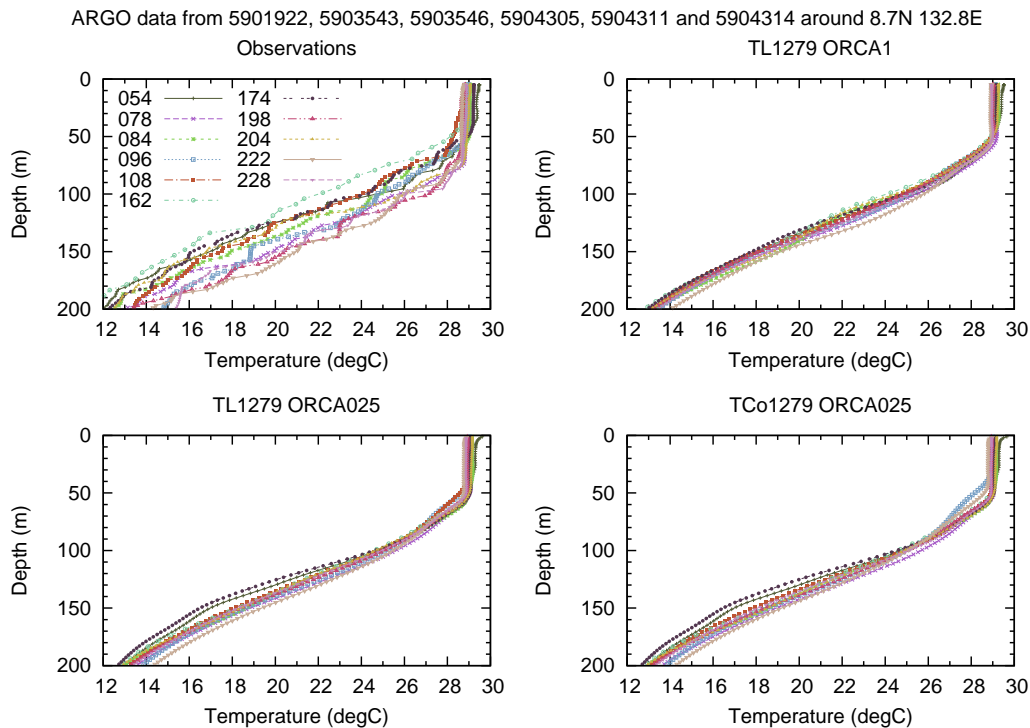
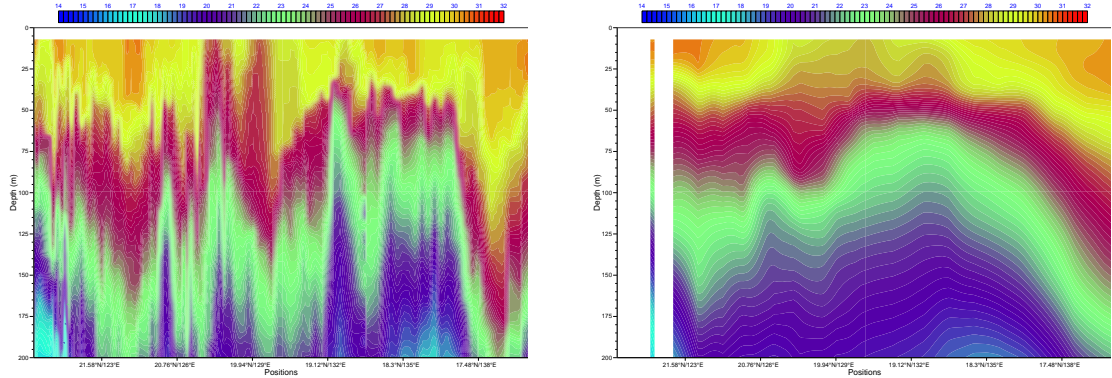


Figure 13: Vertical temperature profiles from different Argo observations compared to forecasts made with different atmospheric and oceanographic resolutions (indicated on the top of each plot) starting from 2013-11-04 00 UTC. Each curve is for a different forecast lead time (indicated on the plots) corresponding to the valid time of the observations.

point from the different atmospheric and oceanographic resolution coupled model runs starting from 2013110400. Each curve corresponds to a different forecast lead time relative to the start date as indicated on the plots. The data were taken from the EN4 dataset (Good et al., 2013).

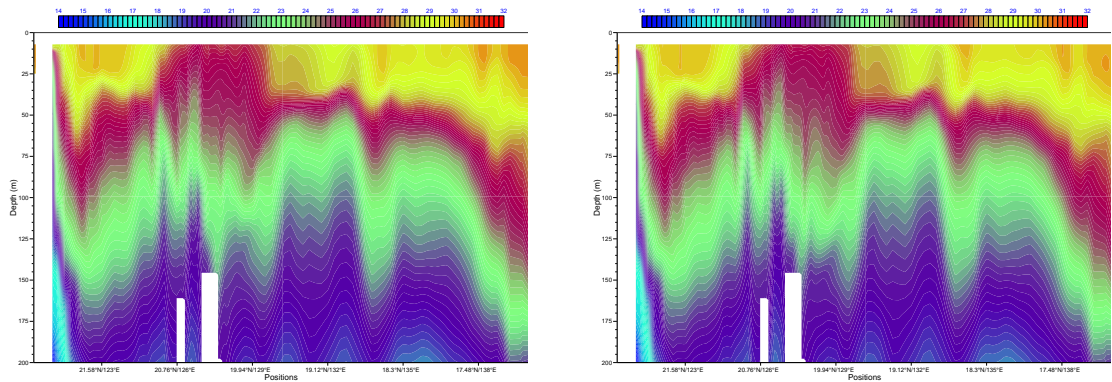
All the different model configurations have a reasonably good mixed layer depth and slope of the thermocline compared to the observations. However, we see more temporal variability in the observations than in any of the different model configurations. Using the temporal variation of depth at a given isotherm (e.g. 18°C) as an estimate of the amplitude of the internal wave (assuming the temperature changes are dominated by the passage of the tropical cyclone) we see that with increased ocean model resolution the amplitude increases (as also seen on Figure 11), but the amplitude is still less than the observed amplitude (top left panel) for all model configurations. A possible reason for this could be that they all under-predict the intensity of Haiyan, so even if the ocean model was perfect, the response amplitude is expected to be lower than the observed one.

The temperature response modelled for Neoguri is qualitatively similar to that observed under Typhoon Fanapi under ITOP project (D'Asaro et al., 2014), but unfortunately we do not have the observational data for the actual typhoon to confirm that the response is reasonable. The closest observational data we have found in the EN4 data set is a ship deploying expendable bathythermograph's (XBT's) travelling from Taiwan eastwards over the wake of Neoguri as shown in Figure 14. In the plots, only the last half



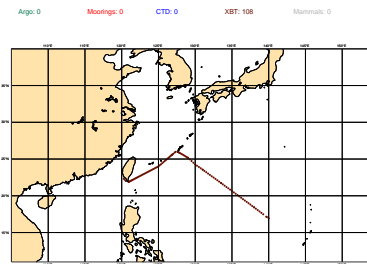
(a) Observations

(b) TL1279 ORCA1



(c) TL1279 ORCA025

(d) TCo1279 ORCA025



(e) Track

Figure 14: Temperature from XBT's launched from ship callsign VF2FE8 after Neoguri. Upper left the is observed temperature along the track of the ship, upper left, middle left and middle right is the model simulated temperature from a coupled runs with TL1279/ORCA1, TL1279/ORCA025 and TCo1279/ORCA025 atmospheric/oceanographic resolutions respectively. At the bottom is the track of the ship which sailed from west to east.

corresponds to the remains of the ocean response to Neoguri. While there is some similarities between the model runs and the observations for the upwelling and downwelling, it is clear that also for Neoguri the model is unable to simulate the high variability in the observations.

The existence of near-internal waves and subsequent currents in the wake of a tropical storm has been well-established both theoretically and from observations (Shay and Elsberry, 1978; Gill, 1984; Shay et al., 1992; Ginis, 2002). For both Haiyan (Figure 11, bottom 3 panels) and Neoguri (Figure 12, bottom 3 panels), we see the evidence in evolution of the ocean currents of such a wave after the passage of the typhoon. It is a lot stronger for Neoguri, but it is clearly also present in Haiyan simulations. The amplitude of the waves increases with increasing atmospheric/oceanographic resolution, but again it is hard to find observational data to confirm the magnitude.

Since the response for the currents goes to the surface we can use surface currents as a proxy for the response to quantify if the oceanographic response is reasonable. In Figure 15 is shown the currents as derived by Elipot et al. (2016) for the same 4 drifting buoys for which we showed the sea surface temperature evolution in 10. For buoy 52514 on 15(a), there seems to be a remarkable similarity between the model runs and the observations with slight phase error between the observations and the model runs. For the other buoys, the amplitude is too small which is consistent with a too weak response seen in the temperature measurements from the ship (Figure 14). We find an increase in ocean response to the tropical cyclone with increased oceanographic and atmospheric resolution, and while we still seem to be unable to simulate the full magnitude of the interaction with the coupled model configurations used in this study, we are confident that the basic physical mechanism is present and will enable an improvement of the predictions of tropical cyclones compared to the uncoupled model configurations.

5 Discussion

In this report, we have investigated the impact of ocean coupling on tropical cyclone intensity forecasts for different atmospheric and oceanographic resolutions and coupling setups. The aim was to better understand under what conditions it is important to have an interactive ocean as part of the modelling system.

By using a coupled ocean-atmosphere model, the intensity is reduced for cyclones with positive intensity error in the uncoupled model, while the results are close to neutral for cyclones that were too weak. The results show a strong effect from the coupling on intense cyclones in the north-western corner of the basin. However, the result raises the question whether the effect is strong because the cyclones in the uncoupled forecasts are very intense (below 950 hPa) or whether this region is more sensitive to ocean coupling (shallower warm layer). If the first statement is the dominant cause, the follow-on question is why the cyclones become stronger in the north-western part of the basin in the forecast compared to other parts.

In this work, we have looked at the sensitivity to model resolutions in both the atmosphere and ocean. For the atmosphere, the impact of resolution was tested for the same set of cases as in Rodwell et al. (2015). By increasing the resolution from 16km to 9 km, the average central pressure was around 10 hPa lower with the increased resolution. For some cases (most notable Neoguri) the increase in atmospheric resolution leads to severe over prediction of the intensity for the uncoupled simulations while similar, in terms of atmospheric resolution, coupled simulations are much better.

The comparison of the upper ocean of the Haiyan and Neoguri predictions lead to the conclusion that knowledge of the vertical stratification of the ocean is crucial to being able to predict the coupled feed-

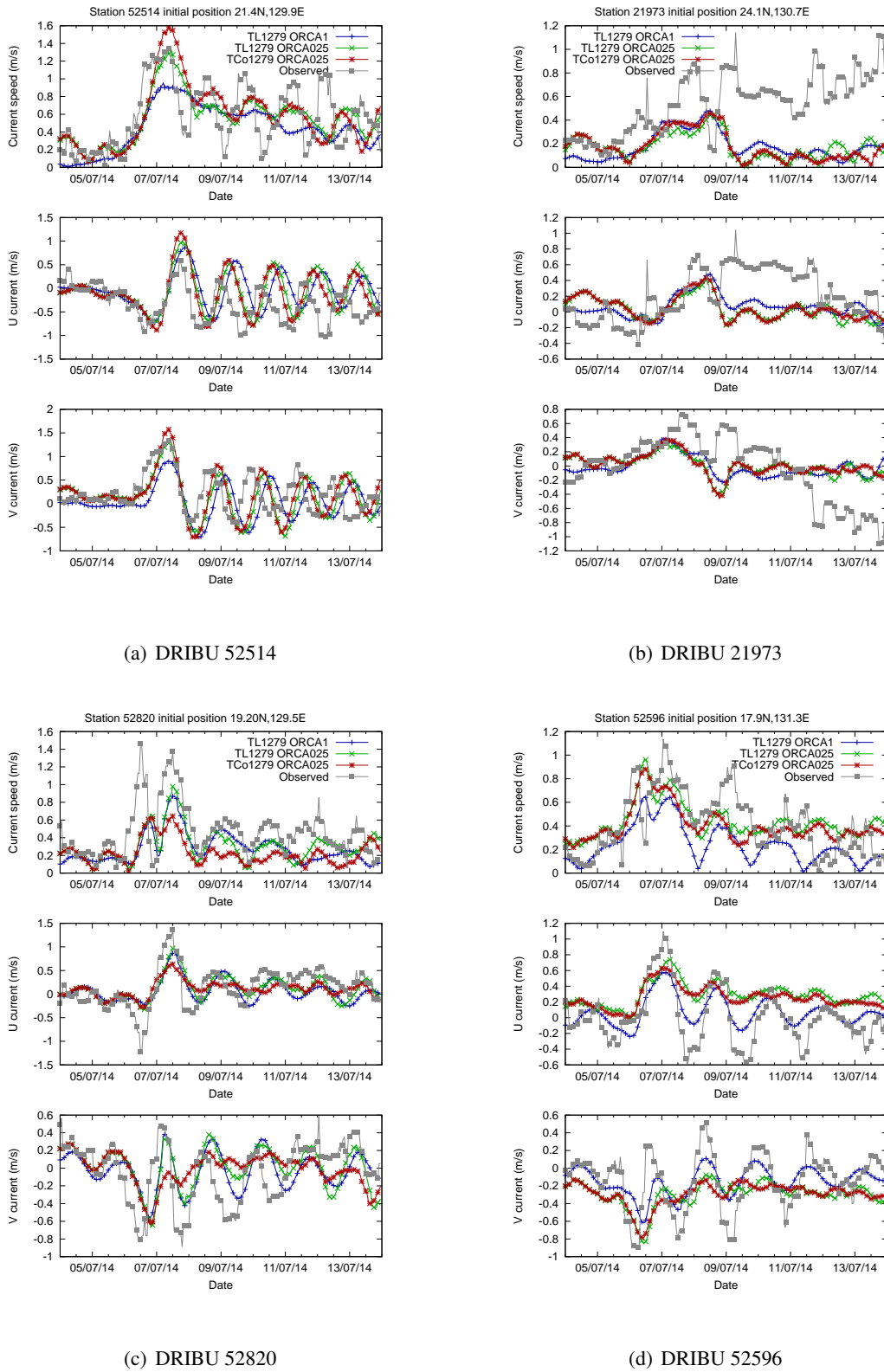


Figure 15: Current forecasts and observations based on *Elipot et al. (2016)* from the same 4 DRIBU as in Figure 10 for the Neoguri case for the different atmospheric and oceanographic resolutions.

back and thereby predict the evolution of the tropical cyclone. For Neoguri we have shown that a shallow warm layer is the key to a strong coupled response whereas for Haiyan the thick warm layer leads to a weak coupled response. The sea surface temperature was actually warmer for the Neoguri case compared to the Haiyan case, but we have shown that the ocean stratification is the main determining factor for the magnitude of the coupled response.

In order to validate the fidelity of the coupling between the atmosphere and the ocean we have looked at the ocean response to the tropical cyclone forcing. The internal waves generated in the ocean in the coupled model looks plausible while not directly verifiable. Indirect verification via comparison with surface currents from drifters gives us confidence that the modelled ocean response is very realistic. Combined with modelled atmospheric response discussed above this makes us confident that the *coupled* model is more realistic for these conditions and would improve the forecasting capabilities of ECMWF if implemented in the currently uncoupled HRES forecasting system.

Our results qualitatively agree with the findings in Ito et al. (2015) where forecasts for 34 tropical cyclones south of Japan were compared between the operational JMA model with 20 km resolution and a non-hydrostatic limited-area model with resolution of 5 km. The intensity error increased (too intense) by using the 5 km model compared to 20 km but was improved by using the coupled high-resolution model.

We have used a set of cases to test the impact of the ocean coupling. However, the effect of the ocean is dependent on the parameterisations of the heat, moisture and momentum exchange between the atmosphere and ocean by the waves. In a similar way as the effect of interactive ocean has been investigated here, the effect of different wave parameterisations could be tested.

References

- Balmaseda, M. A., K. Mogensen, and A. T. Weaver, 2013: Evaluation of the ECMWF ocean reanalysis system ORAS4. *Q. J. R. Met. Soc.*, 1132–1161.
- Breivik, Ø., K. Mogensen, J.-R. Bidlot, M. A. Balmaseda, and P. A. E. M. Janssen, 2015: Surface wave effects in the NEMO ocean model: Forced and coupled experiments. *Journal of Geophysical Research: Oceans*, **120** (4), 2973–2992, doi:10.1002/2014JC010565, URL <http://dx.doi.org/10.1002/2014JC010565>.
- D’Asaro, E., et al., 2014: Impact of Typhoons on the Ocean in the Pacific. *Bulletin of the American Meteorological Society*, **95** (9), 1405–1418, doi:10.1175/BAMS-D-12-00104.1.
- Donlon, C. J., M. Martin, J. Stark, J. Roberts-Jones, E. Fiedler, and W. Wimmer, 2012: The Operational Sea Surface Temperature and Sea Ice Analysis (OSTIA) system. *Remote Sensing of Environment*, **116**, 140 – 158, doi:http://dx.doi.org/10.1016/j.rse.2010.10.017, URL <http://www.sciencedirect.com/science/article/pii/S0034425711002197>, advanced Along Track Scanning Radiometer(AATSR) Special Issue.
- Dvorak, V. F., 1975: Tropical Cyclone Intensity Analysis and Forecasting from Satellite Imagery. *Mon. Wea. Rev.*, **103**, 420–430, doi:10.1175/1520-0493(1975)103<0420:TCIAAF>2.0.CO;2.
- Elipot, S., R. Lumpkin, R. C. Perez, J. M. Lilly, J. J. Early, and A. M. Sykulski, 2016: A global surface drifter data set at hourly resolution. *Journal of Geophysical Research: Oceans*, **121** (5), 2937–2966, doi:10.1002/2016JC011716, URL <http://dx.doi.org/10.1002/2016JC011716>.

- Gill, A. E., 1984: On the Behaviour of Internal Waves in the Wakes of Storms. *J. Phys. Oceano.*, 1129–1151.
- Ginis, I., 2002: Tropical Cyclone-Ocean Interactions. *Atmosphere-Ocean Interactions, Advances in Fluid Mechanics Series*, 83–114.
- Good, S. A., M. J. Martin, and N. A. Rayner, 2013: EN4: Quality controlled ocean temperature and salinity profiles and monthly objective analyses with uncertainty estimates. *Journal of Geophysical Research: Oceans*, **118** (12), 6704–6716.
- Haiden, T., M. Janousek, P. Bauer, J. Bidlot, L. Ferranti, T. Hewson, F. Prates, and D. S. Richardson, 2014: Evolution of ECMWF forecasts, including 2013-2014 upgrades. Technical Memorandum 742, ECMWF.
- Halliwell, G. R., S. Gopalakrishnan, F. Marks, and D. Willey, 2015: Idealized Study of Ocean Impacts on Tropical Cyclone Intensity Forecasts. *Mon. Wea. Rev.*, **143**, 1142–1165, doi:10.1175/MWR-D-14-00022.1.
- Heo, K.-Y., T. Ha, and K.-S. Park, 2017: The effects of a typhoon-induced oceanic cold wake on typhoon intensity and typhoon-induced ocean waves. *Journal of Hydro-environment Research*, **14**, 61 – 75.
- Ito, K., T. Kuroda, and K. Saito, 2015: Forecasting a large number of tropical cyclone intensities around Japan using a high-resolution atmosphere-ocean coupled model. *Wea. Forecasting*, **30**, 793–808, doi:10.1175/WAF-D-14-00034.1.
- Janssen, P. A. E. M., et al., 2013: Air-sea interaction and surface waves. Technical Memorandum 712, ECMWF.
- Knapp, K. R., M. C. Kruk, D. H. Levinson, and C. J. Diamond, H. J. Neumann, 2010: The International Best Track Archive for Climate Stewardship (IBTrACS). *BAMS*, **91**, 363–376, doi:10.1175/2009BAMS2755.1.
- Landsea, C. W. and J. L. Franklin, 2013: Atlantic Hurricane Database Uncertainty and Presentation of a New Database Format. *Mon. Wea. Rev.*, **141**, 3576–3592, doi:10.1175/MWR-D-12-00254.1.
- Levinson, D. H., H. J. Diamond, K. R. Knapp, M. C. Kruk, and E. J. Gibney, 2010: Toward a Homogenous Global Tropical Cyclone Best-Track Dataset. *BAMS*, **91**, 277–280, doi:10.1175/2010BAMS2930.1.
- Lin, I.-I. and C.-C. Pun, I.-F. and Wu, 2009: Upper-Ocean Thermal Structure and the Western North Pacific Category 5 Typhoons. Part II: Dependence on Translation Speed. *Mon. Wea. Rev.*, **137**, 3744–3757, doi:10.1175/2009MWR2713.1.
- Lin, I.-I., I.-F. Pun, and C.-C. Lien, 2014: 'Category-6' supertyphoon Haiyan in global warming hiatus: Contribution from subsurface ocean warming. *Geophys. Res. Lett.*, **41**, 8547–8552.
- Lin, I.-I., C.-C. Wu, I.-F. Pun, and D.-S. Ko, 2008: Upper-Ocean Thermal Structure and the Western North Pacific Category 5 Typhoons. Part I: Ocean Features and the Category 5 Typhoons Intensification. *Mon. Wea. Rev.*, **136**, 3288–3306, doi:10.1175/2008MWR2277.1.
- Madec, G., 2008: *NEMO ocean engine*. France, Note du Pôle de modélisation, Institut Pierre-Simon Laplace (IPSL), no 27, issn no 1288-1619 ed.

- Martin, J. D. and W. M. Grey, 1993: Tropical Cyclone Observation and Forecasting with and without Aircraft Reconnaissance. *Wea. Forecasting*, **8**, 519–532, doi:10.1175/1520-0434(1993)008<0519:TCOAFW>2.0.CO;2.
- Mogensen, K., M. Alonso Balmaseda, and A. Weaver, 2012a: The NEMOVAR ocean data assimilation system as implemented in the ECMWF ocean analysis for System 4. Technical Memorandum 668, ECMWF.
- Mogensen, K., S. Keeley, and P. Towers, 2012b: Coupling of the NEMO and IFS models in a single executable. Technical Memorandum 673, ECMWF.
- Rodwell, M. J., et al., 2015: New developments in the diagnosis and verification of high-impact weather forecasts. Technical Memorandum 759, ECMWF.
- Sakaïda, F., H. Kawamura, and Y. Toba, 1998: Sea surface cooling caused by typhoons in the Tohoku area in August 1989. *Journal of Geophysical Research: Oceans*, **103 (C1)**, 1053–1065.
- Shay, L. K., P. G. Black, M. A. J., J. D. Hawkins, and R. L. Elsberry, 1992: Upper Ocean Response to Hurricane Gilbert. *J. Geophys. Res.*, 20 227–20 248.
- Shay, L. K. and R. L. Elsberry, 1978: Near-Inertial Ocean Current Response to Hurricane Frederic. *J. Phys. Oceano.*, 1249–1269.
- Takaya, Y., F. Vitart, G. Balsamo, M. Balmaseda, M. Leutbecher, and F. Molteni, 2010: Implementation of an ocean mixed layer model in IFS. Technical Memorandum 622, ECMWF.
- Velden, C., et al., 2006: The Dvorak Tropical Cyclone Intensity Estimation Technique: A Satellite-Based Method that Has Endured for over 30 Years. *Bull. Amer. Meteor. Soc.*, **87**, 1195–1210, doi:10.1175/BAMS-87-9-1195.
- Wada, A., T. Uehara, and S. Ishizaki, 2014: Typhoon-induced sea surface cooling during the 2011 and 2012 typhoon seasons: observational evidence and numerical investigations of the sea surface cooling effect using typhoon simulations. *Progress in Earth and Planetary Science*, **1 (1)**, 11.
- Wedi, N. P., et al., 2015: The modelling infrastructure of the Integrated Forecasting System: Recent advances and future. Technical Memorandum 760, ECMWF.
- Yablonsky, R. M. and I. Ginis, 2009: Limitation of One-Dimensional Ocean Models for Coupled Hurricane-Ocean Model Forecasts. *Mon. Wea. Rev.*, **139**, 4410–4419, doi:10.1175/2009MWR2863.1.
- Zuo, H., M. A. Balmaseda, and K. Mogensen, 2015: The new eddy-permitting orap5 ocean reanalysis: description, evaluation and uncertainties in climate signals. *Climate Dynamics*, 1–21, doi:10.1007/s00382-015-2675-1, URL <http://dx.doi.org/10.1007/s00382-015-2675-1>.